# Relativistic Quantum Brayton Engine Based on Two Non-Interacting Dirac Particles in a One-Dimensional Potential Well

Titis Qorin Nabila*, Heru Sukamto, and Agus Purwanto
*Department of Physics, Faculty of Science and Analytical Data*
*Institut Teknologi Sepuluh Nopember, Kampus ITS Sukolilo, Surabaya 60111*

**Abstract**: A quantum heat engine converts heat into work based on the principles of quantum thermodynamics.This study investigates a quantum heat engine composed of two Dirac particles confined in a one-dimensional potential well. The potential well is limited to three discrete energy levels, and the two non-interacting Dirac particles are treated as identical. The system operates under a quantum Brayton cycle, consisting of isobaric and adiabatic processes. The total work output is calculated using the energy levels derived from the relativistic Dirac equation. The efficiency curve is obtained by plotting a theoretical expression as a function of the ratio $L_A/\lambda$, where $\lambda$ is the Compton wavelength. The efficiency increases monotonically with $L_A/\lambda$, approaching an asymptotic maximum, and is further enhanced by larger values of the parameter $\alpha$, which drive the engine toward near-optimal performance.

Keywords: Brayton Cycle; Dirac Particle; Eficiency; Potential Well.

*Corresponding author: titisqorin21@gmail.com

http://dx.doi.org/10.12962/j24604682.v21i3.22945
2460-4682 

## I. INTRODUCTION

Similar to classical thermodynamics, quantum thermodynamics also introduces the concept of a quantum heat engine. Its main principle is the conversion of heat into work by utilizing quantum systems as the working medium. These engines operate through thermodynamic cycles, among which the Brayton cycle comprising isobaric and adiabatic processes is widely studied. This cycle was introduced by John Barber in 1791 and further developed by George Brayton [1].

Quantum thermodynamic quantities have analogies with quantities in classical thermodynamics. For instance, pressure corresponds to force, volume to system length, and internal energy to the expectation value of the Hamiltonian operator. Heat energy is associated with a probability change in the expectation value of the Hamiltonian, while work is associated with a change in the eigenenergy of the system [2].

The operation of quantum heat engines is governed by the laws of quantum thermodynamics. The change in internal energy is given by:

$$dU = dQ - dW. \tag{1}$$

where the infinitesimal heat and work are defined as:

$$dQ = \sum_n E_n \, dP_n, \quad dW = \sum_n P_n \, dE_n, \tag{2}$$

This equation is an implication of the first law of thermodynamics [3].

According to the second law of thermodynamics, the efficiency of a heat engine is defined as the ratio of the work performed to the input heat:

$$\eta = \frac{W}{Q_{\text{in}}} \tag{3}$$

Where $\eta$ is the efficiency, $W$ is the total work, and $Q_{in}$ is the incoming heat. This law also confirms that the efficiency of the engine cannot reach 100 percent [4].

Research on quantum heat engines has progressed rapidly, particularly in exploring various types of working media.

Research on quantum heat engines has grown rapidly, especially related to variations in the working medium used. One of the working mediums that is often studied is potential wells [5]. In this paper, the efficiency of a quantum heat engine using two Dirac particles in a one-dimensional potential well operating on a Brayton cycle is examined in detail. The potential well under consideration has three available energy levels. Since Dirac particles are fermions, they obey the Pauli exclusion principle, which states that no two fermions can occupy the same quantum state simultaneously. Consequently, each energy level in the potential well can be occupied by only one of the two Dirac particles.

This paper is organized as follows. Section II discusses the energy solution for a single Dirac particle in a potential well, beginning with the Dirac equation and detailing the derivation steps that lead to the energy solution. Section III introduces the concept of a quantum heat engine based on this system, operating according to the Brayton cycle. This section also presents the formulation of heat input and output for the quantum heat engine. Section IV describes the efficiency formula of the quantum heat engine and presents the corresponding efficiency graph.

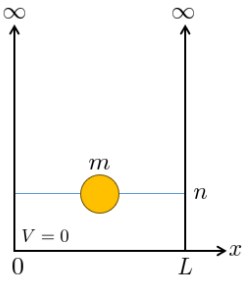


FIG. 1: A Dirac particle in a one-dimensional infinite potential well.

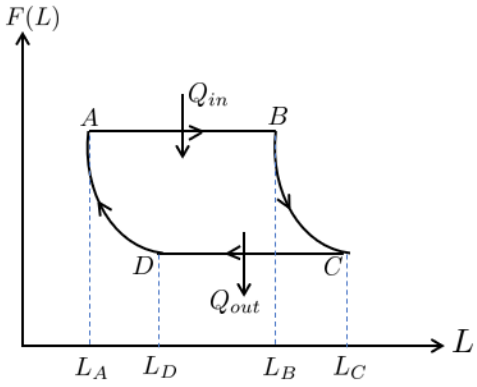


FIG. 2: Brayton Cycle

## II. ENERGY SOLUTION FOR A DIRAC PARTICLE IN A ONE-DIMENSIONAL POTENTIAL WELL

We consider a Dirac particle of mass $m$ confined in a one-dimensional infinite potential well of width $L$. The potential outside the well is infinite, while it is zero inside the well. A schematic of this system is shown in Figure 1.

To determine the energy spectrum of the Dirac particle, we begin with the Dirac equation:

$$E\psi = \left(c\vec{\alpha}\cdot\vec{p} + \beta mc^2\right)\psi, \tag{4}$$

where $\vec{\alpha} = (\alpha_1, \alpha_2, \alpha_3)$ are the Dirac matrix defined as:

$$\alpha_i = \begin{pmatrix} 0 & \sigma_i \\ \sigma_i & 0 \end{pmatrix}, i = 1, 2, 3, \tag{5}$$

with $\sigma_i$ being the Pauli matrices:

$$\sigma_1 = \begin{pmatrix} 0 & 1 \\ 1 & 0 \end{pmatrix}, \quad \sigma_2 = \begin{pmatrix} 0 & -i \\ i & 0 \end{pmatrix}, \quad \sigma_3 = \begin{pmatrix} 1 & 0 \\ 0 & -1 \end{pmatrix}. \tag{6}$$

The $\beta$ matrix is defined as:

$$\beta = \begin{pmatrix} I & 0 \\ 0 & -I \end{pmatrix}, \tag{7}$$

and $\psi$ is written as:

$$\psi = \begin{pmatrix} \eta \\ \chi \end{pmatrix} \tag{8}$$

with

$$\eta = \begin{pmatrix} \psi_1 \\ \psi_2 \end{pmatrix}, \text{and} \quad \chi = \begin{pmatrix} \psi_3 \\ \psi_4 \end{pmatrix}. \tag{9}$$

$\psi_1$, $\psi_2$, $\psi_3$, dan$\psi_4$ are spinors [6].

By substituting Eqs. (5)(8) into the Dirac equation (4), and considering the one-dimensional case, we obtain the following second-order differential equation:

$$\frac{d^2\eta}{dx^2} + k^2\eta = 0, \tag{10}$$

with the general solution:

$$\eta = A\cos(kx) + B\sin(kx), \tag{11}$$

where the wavenumber $k$ is defined as:

$$k^2 = \frac{E^2 - m^2c^4}{c^2\hbar^2}. \tag{12}$$

To find the quantized energy levels, we apply the boundary conditions:

$$V(x) = \begin{cases} 0, & 0 \le x \le L, \\ \infty, & \text{otherwise.} \end{cases} \tag{13}$$

These conditions imply that the wavefunction must vanish at the boundaries, leading to:

$$k = \frac{n\pi}{L}, \quad n = 1, 2, 3, ... \tag{14}$$

Substituting this expression for $k$ into Eq. (12) yields the relativistic energy spectrum:

$$E_n = \sqrt{\left(\frac{n\pi\hbar c}{L}\right)^2 + m^2c^4}. \tag{15}$$

This equation represents the energy levels for a Dirac particle confined in a one-dimensional infinite potential well.

## III. A POTENTIAL WELL WITH TWO DIRAC PARTICLES AS A QUANTUM HEAT ENGINE IN BRAYTON CYCLES

Analogous to the movable piston in classical heat engines, the potential well walls can change dynamically. The potential well is subjected to a thermodynamic Brayton cycle consisting of four distinct processes: adiabatic compression, isobaric expansion, adiabatic expansion, and isobaric compression. [2].

As shown in Figure 2, the Brayton cycle consists of four thermodynamic processes: AB (isobaric expansion), BC (adiabatic expansion), CD (isobaric compression), and DA (adiabatic compression). During each stage of the cycle, the potential well boundaries shift by the corresponding thermodynamic processes. In this model, the potential well contains

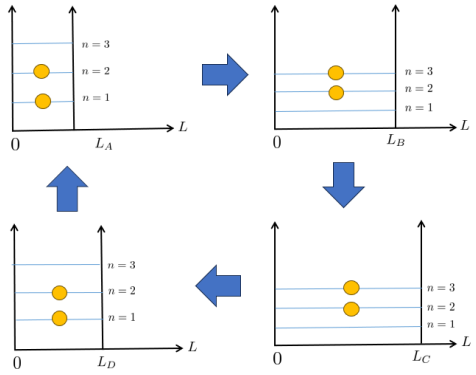


FIG. 3: Schematic representation of two Dirac particles confined in a one-dimensional infinite potential well undergoing state transitions throughout a quantum Brayton cycle.

three discrete energy levels and is occupied by two identical Dirac fermions of mass $m$. Due to the Pauli exclusion principle, the particles occupy different quantum states within the well.

During the isobaric expansion process, both particles are excited, whereas during isobaric compression, they are de-excited. Under the assumption that $W_{BC} - W_{DA} = 0$, the formulation is restricted to the work contributions arising exclusively from the isobaric expansion and compression processes [3]. A more detailed explanation of the work performed during these stages is provided in the following section.

### A. Incoming Heat by Isobaric Expansion

The cycle begins with an isobaric expansion process during which heat is absorbed by the system. During this process, the wall of potential well shifts to the right, from $L_A$ to $L_B$, without any change in the applied force. The constant-force condition during this process is expressed as:

$$F_{AB}(L) = F(L_A) = F(L_B). \tag{16}$$

During this stage, the two Dirac particles, which initially occupy the first and second energy levels, are excited to the second and third levels (see figure 3), respectively, due to the absorbed heat. Based on equation (16) and the definition of force as the derivative of energy with respect to the potential well width:

$$F = \frac{\partial E}{\partial L}, \tag{17}$$

the relationship between the width of the potential well $L_A$ and $L_B$ is obtained as follows:

$$\frac{L_A^3}{L_B^3} = \frac{\frac{1}{\sqrt{\left(\frac{\hbar\pi c}{L_A}\right)^2+m^2c^4}} + \frac{4}{\sqrt{\left(\frac{2\hbar\pi c}{L_A}\right)^2+m^2c^4}}}{\frac{4}{\sqrt{\left(\frac{2\hbar\pi c}{L_B}\right)^2+m^2c^4}} + \frac{9}{\sqrt{\left(\frac{3\hbar\pi c}{L_B}\right)^2+m^2c^4}}}. \tag{18}$$

Using equation (18), the work done during this expansion can be expressed as:

$$\begin{aligned} W_{AB} =& \int_{L_A}^{L_B} F_{AB}(L)\, dL \\ =& \frac{1}{L_B^2}\left(\frac{(2\pi\hbar c)^2}{\sqrt{\left(\frac{2\pi\hbar c}{L_B}\right)^2+m^2c^4}} + \frac{(3\pi\hbar c)^2}{\sqrt{\left(\frac{3\pi\hbar c}{L_B}\right)^2+m^2c^4}}\right) \\ & - \frac{1}{L_A^2}\left(\frac{(\pi\hbar c)^2}{\sqrt{\left(\frac{\pi\hbar c}{L_A}\right)^2+m^2c^4}} + \frac{(2\pi\hbar c)^2}{\sqrt{\left(\frac{2\pi\hbar c}{L_A}\right)^2+m^2c^4}}\right). \end{aligned} \tag{19}$$

The change in internal energy resulting from the expansion of the well width from $L_A$ to $L_B$ is given by:

$$\begin{aligned} \Delta U_{AB} =& E(L_B) - E(L_A) \\ =& \sqrt{\left(\frac{2\pi\hbar c}{L_B}\right)^2+m^2c^4} + \sqrt{\left(\frac{3\pi\hbar c}{L_B}\right)^2+m^2c^4} \\ & - \sqrt{\left(\frac{\pi\hbar c}{L_A}\right)^2+m^2c^4} + \sqrt{\left(\frac{2\pi\hbar c}{L_A}\right)^2+m^2c^4}. \end{aligned} \tag{20}$$

The heat absorbed by the system during the isobaric expansion, obtained by summing equations (19) and (20), is:

$$\begin{aligned} Q_{in} =& W_{AB} + \Delta U_{AB} \\ =& \frac{2(2\pi\hbar c)^2 + m^2L_B^2c^4}{L_B^2\sqrt{\left(\frac{2\pi\hbar c}{L_B}\right)^2+m^2c^4}} + \frac{2(3\pi\hbar c)^2 + m^2L_B^2c^4}{L_B^2\sqrt{\left(\frac{3\pi\hbar c}{L_B}\right)^2+m^2c^4}} \\ & - \frac{2(\pi\hbar c)^2 + m^2L_A^2c^4}{L_A^2\sqrt{\left(\frac{\pi\hbar c}{L_A}\right)^2+m^2c^4}} - \frac{2(2\pi\hbar c)^2 + m^2L_A^2c^4}{L_B^2\sqrt{\left(\frac{2\pi\hbar c}{L_A}\right)^2+m^2c^4}}. \end{aligned} \tag{21}$$

The Compton wavelength of a particle is $\lambda = \frac{2\pi\hbar}{mc}$ [7], allowing equation (21) to be rewritten in terms of $\lambda/L_A$ and $\lambda/L_B$ as follows:

$$\begin{aligned} Q_{in} =& mc^2\left(\frac{2\left(\frac{\lambda}{L_B}\right)^2+1}{\sqrt{\left(\frac{\lambda}{L_B}\right)^2+1}} + \frac{\frac{9}{2}\left(\frac{\lambda}{L_B}\right)^2+1}{\sqrt{\frac{9}{4}\left(\frac{\lambda}{L_B}\right)^2+1}}\right. \\ & \left. - \frac{\frac{1}{2}\left(\frac{\lambda}{L_A}\right)^2+1}{\sqrt{\frac{1}{4}\left(\frac{\lambda}{L_A}\right)^2+1}} - \frac{2\left(\frac{\lambda}{L_A}\right)^2+1}{\sqrt{\left(\frac{\lambda}{L_A}\right)^2+1}}\right). \end{aligned} \tag{22}$$

After this stage, the cycle proceeds to the adiabatic expansion process, during which no heat is exchanged with the surroundings [8].

### B. Heat Released by Isobaric Compression

This stage corresponds to the third step of the cycle, where heat is released through an isobaric compression process [3].In this stage, the wall of the potential well moves, resulting in a change in width from $L_C$ to $L_D$ under constant force.

The constant force during this process is given by:

$$F_{CD}(L) = F(L_C) = F(L_D). \tag{23}$$

During this process, two Dirac particles undergo de-excitation. Initially occupying the second and third energy levels, they transition to the first and second levels (see figure 3), respectively, as heat is released from the system. The relationship between well widths $L_C$ and $L_D$ can be written as:

$$\frac{L_C^3}{L_D^3} = \frac{\frac{4}{\sqrt{\left(\frac{2\hbar\pi c}{L_C}\right)^2+m^2c^4}} + \frac{9}{\sqrt{\left(\frac{3\hbar\pi c}{L_C}\right)^2+m^2c^4}}}{\frac{1}{\sqrt{\left(\frac{\hbar\pi c}{L_D}\right)^2+m^2c^4}} + \frac{4}{\sqrt{\left(\frac{2\hbar\pi c}{L_D}\right)^2+m^2c^4}}}. \tag{24}$$

As in isobaric expansion, the isobaric compression process also produces work which is calculated as:

$$\begin{aligned} W_{CD} =& \int_{L_C}^{L_D} F_{CD}(L)\, dL \\ =& \frac{1}{L_D^2}\left(\frac{(\pi\hbar c)^2}{\sqrt{\left(\frac{\pi\hbar c}{L_D}\right)^2+m^2c^4}} + \frac{(2\pi\hbar c)^2}{\sqrt{\left(\frac{2\pi\hbar c}{L_D}\right)^2+m^2c^4}}\right) \\ & - \frac{1}{L_C^2}\left(\frac{(2\pi\hbar c)^2}{\sqrt{\left(\frac{2\pi\hbar c}{L_C}\right)^2+m^2c^4}} + \frac{(3\pi\hbar c)^2}{\sqrt{\left(\frac{3\pi\hbar c}{L_C}\right)^2+m^2c^4}}\right). \end{aligned} \tag{25}$$

The change in internal energy due to the change in well width from $L_C$ to $L_D$ can be written as:

$$\begin{aligned} \Delta U_{CD} =& E(L_D) - E(L_C) \\ =& \sqrt{\left(\frac{\pi\hbar c}{L_D}\right)^2+m^2c^4} + \sqrt{\left(\frac{2\pi\hbar c}{L_D}\right)^2+m^2c^4} \\ & - \sqrt{\left(\frac{2\pi\hbar c}{L_C}\right)^2+m^2c^4} - \sqrt{\left(\frac{3\pi\hbar c}{L_C}\right)^2+m^2c^4}. \end{aligned} \tag{26}$$

Using equations (25) and (26), the amount of heat escaping from the system during the isobaric compression process can be calculated as:

$$\begin{aligned} Q_{out} =& W_{CD} + \Delta U_{CD} \\ =& \frac{2(\pi\hbar c)^2 + m^2L_D^2c^4}{L_D^2\sqrt{\left(\frac{\pi\hbar c}{L_D}\right)^2+m^2c^4}} + \frac{2(2\pi\hbar c)^2 + m^2L_D^2c^4}{L_D^2\sqrt{\left(\frac{2\pi\hbar c}{L_D}\right)^2+m^2c^4}} \\ & - \frac{2(2\pi\hbar c)^2 + m^2L_C^2c^4}{L_C^2\sqrt{\left(\frac{2\pi\hbar c}{L_C}\right)^2+m^2c^4}} - \frac{2(3\pi\hbar c)^2 + m^2L_C^2c^4}{L_C^2\sqrt{\left(\frac{3\pi\hbar c}{L_C}\right)^2+m^2c^4}}. \end{aligned} \tag{27}$$

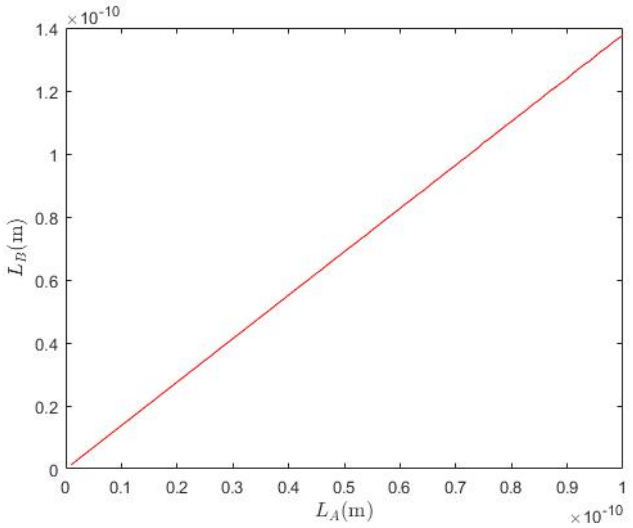


FIG. 4: Relationship between $L_A$ and $L_B$ obtained from the Monte Carlo method.

As with the isobaric expansion, the above expression can be rewritten in terms of $\lambda/L_C$ and $\lambda/L_D$:

$$\begin{aligned} Q_{out} =& mc^2\left(\frac{\frac{1}{2}\left(\frac{\lambda}{L_D}\right)^2+1}{\sqrt{\frac{1}{4}\left(\frac{\lambda}{L_D}\right)^2+1}} + \frac{2\left(\frac{\lambda}{L_D}\right)^2+1}{\sqrt{\left(\frac{\lambda}{L_D}\right)^2+1}}\right. \\ & \left. - \frac{2\left(\frac{\lambda}{L_C}\right)^2+1}{\sqrt{\left(\frac{\lambda}{L_C}\right)^2+1}} - \frac{\frac{9}{2}\left(\frac{\lambda}{L_C}\right)^2+1}{\sqrt{\frac{9}{4}\left(\frac{\lambda}{L_C}\right)^2+1}}\right). \end{aligned} \tag{28}$$

Following the isobaric compression, the cycle proceeds with an adiabatic compression, thereby returning to the initial state and completing the thermodynamic cycle.

## IV. EFFICIENCY

The work done during the adiabatic processes is neglected; thus, the efficiency of the quantum heat engine is defined as:

$$\eta = 1 - \left|\frac{Q_{out}}{Q_{in}}\right|, \tag{29}$$

where the values of $Q_{in}$ and $Q_{out}$ are given by equations (22) and (28). This efficiency depends on four parameters:$L_A$, $L_B$, $L_C$, and $L_D$. For the purpose of visualization, these dependencies are reduced to two parameters.

The analysis begins with equations (18) and (24), which are recursive in nature. Using the Monte Carlo method, the relationships between $L_A$ and $L_B$, as well as $L_C$ and $L_D$, are determined, as shown in Figures 4 and 5.

Figure 4 shows that the relationship between $L_A$ and $L_B$ is linear with a positive slope of 1.3771. Similarly, Figure 5 reveals a linear relationship between $L_C$ and $L_D$ with a slope

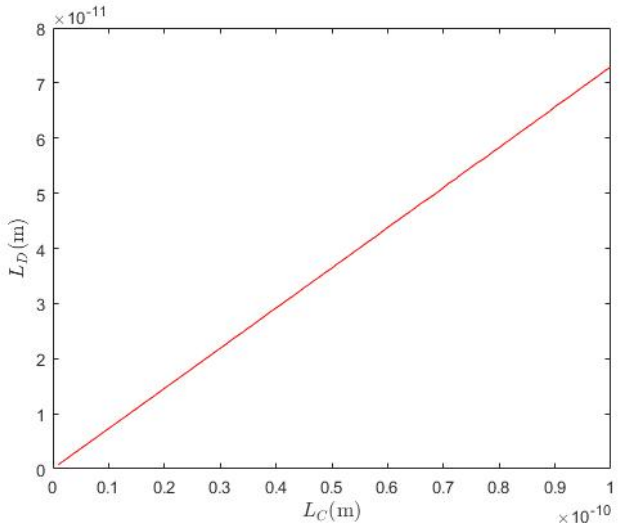


FIG. 5: Relationship between $L_C$ and $L_D$ obtained from the Monte Carlo method.

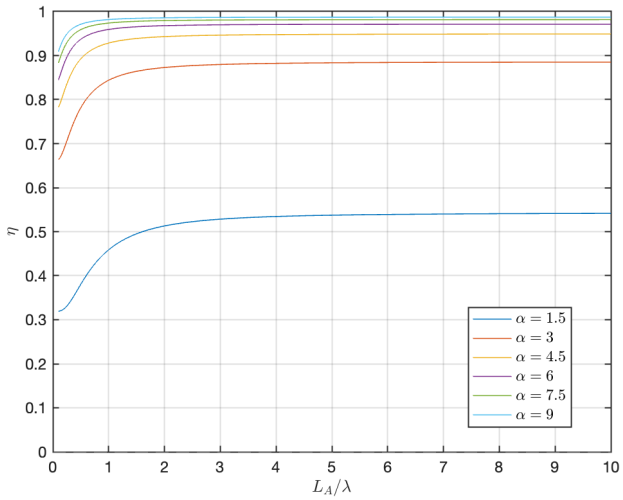


FIG. 6: Efficiency $\eta$ as a function of the length ratio $L_A/\lambda$, showing a monotonically increasing trend approaching an asymptotic limit.

of 0.7304. These ratios satisfy the constraints of the Brayton cycle, where $L_B$ must be greater than $L_A$ and $L_C$ must be less than $L_D$. For further analysis, the substitution $L_A = \alpha L_D$ is introduced, thereby reducing the system to two independent parameters: $\alpha$ and $L_A/\lambda$.

Figure 6 shows the quantum heat engine efficiency as a function of $\frac{L_A}{\lambda}$, for $\alpha$ values ranging from 1.5 to 9. In the range $\frac{L_A}{\lambda} \in [0, 1]$, the efficiency remains low across all values of $\alpha$. However, it increases significantly as $\frac{L_A}{\lambda}$ grows. At this point, the quantum heat engine operates at its maximum efficiency, and further increases in $\frac{L_A}{\lambda}$ yield only marginal improvements.

In the range $\frac{L_A}{\lambda} \in [1, 3]$, the efficiency increase begins to decelerate. Beyond $\frac{L_A}{\lambda} = 3$, the efficiency approaches a stable asymptotic value. At this point, the quantum heat engine operates at its maximum efficiency, and further increases in $\frac{L_A}{\lambda}$ yield only marginal improvements.

The parameyer of $\alpha$ affects the efficiency of the quantum heat engine. Larger values of $\alpha$ lead to both higher average and maximum efficiency. Therefore, a quantum heat engine with larger $\alpha$ exhibits improved capability in converting heat into work.

## V. CONCLUSION

A graph of the efficiency of a relativistic quantum heat engine as a function of $L_A/\lambda$ has been obtained, based on the total work produced by two Dirac particles confined in a one-dimensional potential well undergoing a Brayton cycle. The relationships between $L_A$ and $L_B$, as well as $L_C$ and $L_D$, were determined using the Monte Carlo method. The results show that as $L_A/\lambda$ increases, the efficiency increases monotonically and approaches an asymptotic maximum. Additionally, the parameter $\alpha$ significantly affects the engine's performance, with larger values of $\alpha$ yielding higher average and peak efficiencies. For $\alpha \geq 4.5$, the engine operates with efficiency close to unity, indicating near-optimal performance. Future studies are encouraged to investigate the effect of particle number on the efficiency of relativistic quantum heat engines.

### Acknowledgments

The author would like to thank all colleagues and reviewers whose valuable suggestions have helped improve this work.

[1] N. Ainiyah, *Studi Mesin Brayton Kuantum Berbasis Sistem Partikel Tunggal pada Sumur Potensial Tak Hingga 1 Dimensi dan Sistem Osilator Harmonik*, Jurusan Fisika, Fakultas Sains dan Teknologi, Universitas Islam Negeri Maulana Malik Ibrahim, Malang, 2021.

[2] M. S. Akbar, E. Latifah, and H. Wisodo, "Limit of Relativistic Quantum Brayton Engine of Massless Boson Trapped 1 Dimensional Potential Well," *IOP Conference Series: Journal of Physics*, vol. 1093, p. 012031, 2018.

[3] M. S. Z. R. P. Hasan, *Performa Mesin Panas Kuantum Fraksional Berbasis Partikel pada Kotak 1 Dimensi*, Program Studi Sarjana Fisika, Departemen Fisika, Fakultas Sains dan Analitika Data, Institut Teknologi Sepuluh Nopember, Surabaya, 2024.

[4] F. Abdillah and Y. D. Saputra, "Relativistic quantum-mechanical Brayton engine of the massless boson particle confined in the square well," *AIP Conference Proceedings*, vol. 2296, p. 020118,

2020. doi:10.1063/5.0030870.

[5] H. Sukamto, A. Purwanto, and B. A. Subagyo, "Mesin Panas Kuantum dengan Sistem Multipartikel dan Multi Keadaan," *Jurnal Fisika dan Aplikasinya*, vol. 11, no. 2, pp. -, Juni 2015.

[6] W. Greiner, *Relativistic Quantum Mechanics: Wave Equations*, Springer-Verlag, Berlin, 1990.

[7] E. Muoz and F. J. Pea, "Quantum Heat Engine in the Relativistic Limit: The Case of a Dirac Particle," *Physical Review E*, vol. 86, p. 061108, 2012. DOI: 10.1103/PhysRevE.86.061108.

[8] F. Abdillah, A. Rifani, and Y. D. Saputra, "Quantum Brayton engine based on a single particle in the 2D symmetric potential well," *AIP Conference Proceedings*, vol. 2234, p. 040007, 2020. doi:10.1063/5.0008338.